

JOM 23106

Studies on molybdenocene derivatives: reactions of $[\text{Cp}_2\text{Mo}(\eta^2\text{-NCMe})]$ and preparation of alkyl hydride complexes. Crystal structure of $[\text{Cp}_2\text{Mo}(\text{PMe}_3)]$

Cristina G. de Azevedo^a, M. Arménia A.F. de C.T. Carrondo^b, Alberto R. Dias^a, Ana M. Martins^a, M. Fátima M. Piedade^a and Carlos C. Romão^b

^a Centro de Química Estrutural, Instituto Superior Técnico, 1096 Lisboa Codex (Portugal)

^b Centro de Tecnologia Química e Biológica and Instituto Superior Técnico, R. da Quinta Grande, 6, 2780 Oeiras (Portugal)

(Received May 28, 1992)

Abstract

Reaction of $[\text{Cp}_2\text{Mo}(\eta^2\text{-NCMe})]$ (**1**) with PMe_3 affords $[\text{Cp}_2\text{Mo}(\text{PMe}_3)]$ (**2**), which is readily alkylated to give $[\text{Cp}_2\text{MoR}(\text{PMe}_3)]\text{PF}_6$ (**3a**, R = Me; **3b**, R = Et). The crystal structure of **2** shows tricoordination around the Mo atom. Cyclic voltammetry of **3a** and **3b** and the analogues $[\text{Cp}_2\text{MoR}(\text{CNMe})]\text{I}$, (**4a**, R = Me; **4b**, R = Et) and $[\text{Cp}_2\text{MoMe}(\text{PPh}_3)]\text{PF}_6$ (**7**) shows one reversible one-electron oxidation, but the potential is independent of R, in contrast to the complexes $[\text{Cp}_2\text{MoR}_2]$. Oxidative addition of Et_2S_2 , Ph_2Se_2 or $(\text{PhCO})_2$ to **1** yields $[\text{Cp}_2\text{Mo}(\text{ER})_2]$ (E = O, S or Se). The molybdenocene alkyl hydrides $[\text{Cp}_2\text{Mo}(\text{H})\text{Me}]$ (**5**) and $[\text{Cp}_2\text{MoH}(\text{CH}_2\text{PPh}_3)]\text{I} \cdot \text{THF}$ (**6**) are prepared from $[\text{Cp}_2\text{MoH}]$. Thermal decomposition of **6** as well as reaction of $[\text{Cp}_2\text{MoMe}_2]^+$ with Ph_3C^- provide evidence for transient formation of the methyldene complex $[\text{Cp}_2\text{MoH}(\text{CH}_2)]^+$.

1. Introduction

In previous publications on molybdenocene chemistry we have dealt with the preparation of both low oxidation state complexes, *e.g.* $[\text{Cp}_2\text{MoL}]$ (L = PPh_3 or CNR) [**1**], and alkyl derivatives, *e.g.* $[\text{Cp}_2\text{MoR}_2]$ (R = Et or Bu) [**2**] (Cp = $\eta^5\text{-C}_5\text{H}_5$ throughout the paper). The former electron-rich d^4 complexes readily add to electrophiles E (E = H^+ , R^+ or ML_n) to give $[\text{Cp}_2\text{Mo}(\text{E})\text{L}]^+$ complexes which retain the Mo–L bond. During these studies we found that $[\text{Cp}_2\text{Mo}(\eta^2\text{-NCMe})]$ (**1**) [**3**] is a very convenient starting material for preparation of the complexes $[\text{Cp}_2\text{Mo}(\text{CNR})]$, which could not be reproducibly prepared by the use of reductive methods such as reduction of $[\text{Cp}_2\text{MoX}_2]$ [**4**] and $[\text{Cp}_2\text{MoHL}]^+$ [**1,5**]. In view of the ready preparation of **1**, the easy displacement of the NCMe ligand represents a simple and mild way of generating the Cp_2Mo fragment, which, apart from via the aforementioned reductive routes, has also been obtained by means of thermal and/or photochemical activation of

$[\text{Cp}_3\text{Mo}(\text{CO})]$ [**6**], $[\text{Cp}_2\text{MoH}_2]$ [**7**] or $[\text{Cp}_2\text{Mo}(\text{PEt}_3)]$ [**7e**] and by reductive alkane elimination from $[\text{Cp}_2\text{Mo}(\text{H})\text{R}]$, as has been shown by Cooper *et al.* for $[\text{Cp}_2\text{W}(\text{H})\text{Me}]$ [**8**]. Our method has provided us with a simple preparation of $[\text{Cp}_2\text{Mo}(\text{PMe}_3)]$ (**2**) and the possibility of testing oxidative additions of RE–ER bonds (E = O, S or Se) to Cp_2Mo . A single-crystal X-ray structure determination of **2** is presented together with an electrochemical study of several alkyl cations $[\text{Cp}_2\text{Mo}(\text{R})\text{L}]^+$.

We describe here the complex $[\text{Cp}_2\text{Mo}(\text{H})\text{Me}]$ and provide evidence for transient formation of the alkylidene complexes $[\text{Cp}_2\text{Mo}(\text{CH}_2)\text{R}]^+$ (R = H or Me).

2. Results and discussion

2.1. The complex $[\text{Cp}_2\text{Mo}(\text{PMe}_3)]$ and its derivatives

Treatment of a toluene solution of $[\text{Cp}_2\text{Mo}(\eta^2\text{-NCMe})]$ (**1**) with an excess of PMe_3 at room temperature followed by solvent evaporation and recrystallization from Et_2O gives $[\text{Cp}_2\text{Mo}(\text{PMe}_3)]$ (**2**) in high yield. This highly crystalline orange complex is very air sensitive but can be kept for long periods in solution at room temperature under an inert atmosphere without

Correspondence to: Prof. C. C. Romão.

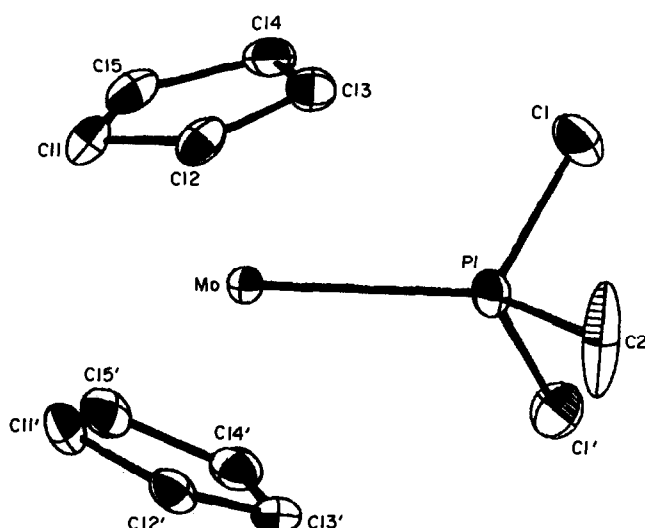


Fig. 1. Molecular structure of $[\text{Cp}_2\text{Mo}(\text{PMe}_3)]$ (**2**) with 50% probability thermal ellipsoids showing the atom-labelling scheme.

noticeable decomposition. This contrasts with the thermal (or photochemical) instability of $[\text{Cp}_2\text{MoPPh}_3]$ under similar conditions. The ^1H nuclear magnetic resonance (NMR) spectrum (Table 1) shows the expected doublets for both the $\eta^5\text{-C}_5\text{H}_5$ and CH_3 protons due to coupling with the ^{31}P nucleus. The coupling constant between the ligand and the ring protons, $^3J(^{31}\text{P}-^1\text{H}) = 4.9$ Hz, is much higher than that usually observed in many cationic complexes $[\text{Cp}_2\text{MoX}(\text{PR}_3)]^+$ [9], *i.e.* about 2 Hz, but is of the same order as the reported values for $[\text{Cp}_2\text{Mo}(\text{PR}_3)]$ ($\text{R} = \text{Et}$ or Ph) [7b,c]. The chemical shift of the Cp protons of these PR_3 derivatives, 3.94 ppm, is one of the lowest found so far for $[\text{Cp}_2\text{MoL}]$ complexes (*e.g.* 4.36 ppm for $\text{L} = \text{CNR}$ [1c] and 4.1 ppm for $\text{L} = \text{C}_2\text{H}_4$ [5b]). This certainly reflects the very high electron density around the metal due to the lack of extensive $\text{Mo} \rightarrow \text{L}$ back donation as found in other $[\text{Cp}_2\text{MoL}]$ complexes with unsaturated π -acidic ligands such as $\text{L} = \text{CO}$ or CNR [1c,6].

The molecular structure of **2** is shown in Fig. 1 and selected bond lengths and bond angles are listed in Table 2. The crystal structure consists of discrete $[\text{Cp}_2\text{Mo}(\text{PMe}_3)]$ molecules with crystallographic mirror symmetry. The molybdenum is coordinated to two Cp rings and to the phosphorus atom of a trimethylphosphine. Mo–P bonds occur in a significant number of biscyclopentadienyl and in monocyclopentadienyl complexes in a variety of coordination geometries. The length of this bond is quite unaffected by the oxidation state of the metal or the type of coordination, as demonstrated by the examples given below. However, typical Mo–P double bonds as observed in $[\text{Cp}_2\text{Mo}(\text{=P}(\text{C}_6\text{H}_2^1\text{Bu}_{3-2,4,6}))]$ [10] (2.370(2) Å) and $[\text{CpMo}(\text{CO})_2(\text{P}(\text{X})(\text{NMe}_2)(\text{CH}_2)_3\text{CMe}_2)]$ [11] (2.214(2) Å for $\text{X} = \text{Cl}$ and 2.243(2) Å for $\text{X} = \text{NMe}_2$) are clearly shorter than single Mo–P bonds.

Examples of biscyclopentadienylmolybdenum(IV) complexes with Mo–P single bonds are $[\text{Cp}_2\text{MoCH}(\text{CF}_3)\text{CH}(\text{CF}_3)\text{PPh}_2]\text{Cl} \cdot \text{H}_2\text{O}$ [13] (2.487(1) Å), $[\text{Cp}_2\text{MoMe}(\text{PPh}_3)_3][\text{PF}_6]$ [1a] (2.526(4) Å) and $[\text{Cp}_2\text{MoH}(\text{PPh}_3)_3][\text{PF}_6]$ [1a] (2.501(4) Å). Related examples of monocyclopentadienylmolybdenum(II) complexes with Mo–P single bonds are $[\text{CpMo}(\text{dppe})(\eta^2\text{-MeC}_2\text{Me})\text{BF}_4]$ [14] (2.442(2) Å), $[\text{CpMo}(\text{CHMe}(\text{PPh}_3))(\text{CO})_2(\text{PPh}_3)]\text{BF}_4$ [15] (2.502(8) Å) and $[\text{CpMo}(\eta^3\text{-CH}_2\text{-CHC=O})(\text{CO})(\text{PPh}_3)]$ [15] (2.509(10) Å).

The Cp ring in $[\text{Cp}_2\text{Mo}(\text{PMe}_3)]$ is planar (maximum deviation 0.0107 Å), with the Mo atom at a distance of 1.932(10) Å from this plane. The angle defined by the normals to the Cp planes is 142.8(3)°. A comparable angle of 144.6° is observed for $[\text{Cp}_2\text{Mo}(\text{=P}(\text{C}_6\text{H}_2^1\text{Bu}_{3-2,4,6}))]$ [10] and 147.7° for $[\text{Cp}_2\text{Mo}(\text{CN}^t\text{Bu})]$ [1c]. However, in tetracoordinated $[\text{MoCp}_2\text{LL}']$ complexes the Cp–Mo–Cp angle is normally smaller, ranging from 128.3(5)° to 139.2(3)° (see ref. 1c and references cited therein).

As mentioned above, electrophilic addition to the metal is the general reactivity pattern found for the

TABLE 1. ^1H NMR spectroscopic data

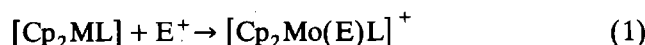
Complex	δ (ppm), multiplicity, relative area, $^nJ(\text{AX})$ (Hz), assignment
$[\text{Cp}_2\text{Mo}(\text{PMe}_3)]$ (2) ^a	3.94 (d, 10, $^3J(^{31}\text{P}-^1\text{H}) = 4.9$, Cp); 0.97 (d, 9, $^3J(^{31}\text{P}-^1\text{H}) = 8.1$, PMe_3)
$[\text{Cp}_2\text{MoMe}(\text{PMe}_3)]\text{PF}_6$ (3a) ^b	5.27 (d, 10, $^3J(^{31}\text{P}-^1\text{H}) = 2.8$, Cp); 1.65 (d, 9, $^3J(^{31}\text{P}-^1\text{H}) = 8.8$, PMe_3); –0.04 (d, 3, $^3J(^{31}\text{P}-^1\text{H}) = 8.9$, Mo–Me)
$[\text{Cp}_2\text{MoEt}(\text{PMe}_3)]\text{PF}_4$ (3b) ^b	5.27 (d, 10, $^3J(^{31}\text{P}-^1\text{H}) = 2.8$, Cp); 1.65 (d, 9, $^3J(^{31}\text{P}-^1\text{H}) = 10.9$, PMe_3); 1.21 (t, 3, $^3J(^1\text{H}-^1\text{H}) = 7.2$, CH_3); 1.00 (dq, 2, $^3J(^1\text{H}-^1\text{H}) = 7.2$, $^3J(^{31}\text{P}-^1\text{H}) = 7.2$, Mo– CH_2)
$[\text{Cp}_2\text{Mo}(\text{H})\text{Me}]$ (5) ^c	4.32 (s, 10, Cp); 0.32 (s, 3, Me); –8.89 (s, 1, H)
$[\text{Cp}_2\text{Mo}(\text{H})\text{CH}_2\text{PPh}_3]\text{I}(\text{THF})$ (6) ^d	7.75–7.60 (m, 15, Ph); 4.54 (s, 10, Cp); 3.63 (t, 4, $^3J(^1\text{H}-^1\text{H}) = 6.2$, $\text{OCH}_2(\text{CH}_2)_2\text{CH}_2$); 1.46 (d, 2, $^2J(^{31}\text{P}-^1\text{H}) = 12.2$, $\text{CH}_2\text{-PPh}_3$); 1.19 (t, 4, $^3J(^1\text{H}-^1\text{H}) = 6.2$, $\text{OCH}_2(\text{CH}_2)_2\text{CH}_2$); –8.05 (d, 1, $^3J(^{31}\text{P}-^1\text{H}) = 7.9$, H)

^a C_6D_6 , 80 MHz, room temperature (Rt); ^b acetone- d_6 , 300 MHz, Rt; ^c toluene- d_3 , 100 MHz, –30°C; ^d CD_3CN , 100 MHz, RT. s, singlet; d, doublet; t, triplet; q, quartet.

TABLE 2. Selected bond lengths (Å) and bond angles (°) for [Cp₂Mo(PMe₃)]

Mo(1)–P(1)	2.468(3)	Mo(1)–Cp	1.932(6)
P(1)–C(1)	1.831(6)	P(1)–C(2)	1.818(10)
C(1)–P(1)–Mo(1)	118.8(2)	C(2)–P(1)–Mo(1)	118.0(3)
C(2)–P(1)–C(1)	99.0(4)	Cp–Mo(1)–Cp'	142.8(3)
P(1)–Mo(1)–Cp	108.6(2)		

electron-rich d⁴ complexes [Cp₂ML] (M = Mo or W) [1a,c,5b]:



Complex **2** exhibits similar reactivity and the alkyl derivatives [Cp₂MoR(PMe₃)]PF₆ (**3a**, R = Me; **3b**, R = Et) are isolated in high yields from reaction of **2** with RI followed by treatment with aqueous NH₄PF₆ and recrystallization.

The ¹H NMR spectra (Table 1) show the expected pattern, with ³¹P–¹H coupling being observed for all types of protons, *i.e.* η⁵-C₅H₅, P–CH₃ and Mo–CH₃. The chemical shifts of the Cp protons and their coupling constants with ³¹P are in the range normally found for this type of cationic complex.

In a previous paper we discussed the electrochemistry of the dialkyl complexes [Cp₂MoR₂] (R = Me, Et or Bu) [2] and found an order of redox potentials with alkyl opposite to that due to inductive effects. In order to compare trends, we studied the electrochemistry of the cationic alkyl complexes **3a** and **3b** and their methylnocyanide analogues [Cp₂MoR(CNMe)]PF₆ (**4a**, R = Me; **4b**, R = Et) [1c]. The cyclic voltammograms are summarized in Table 3.

Within the solvent limits (–1.5 to 1.6 V; CH₃CN) only one reversible oxidation wave was observed for scans between 10 and 500 mV s^{–1}. This oxidation is assigned to the formation of the molybdenum(V) species [Cp₂MoR(L)]²⁺. The order of the oxidation potentials is, however, the one expected on the basis of normal considerations of ligand σ donor capability. The PMe₃ complexes are easier to oxidize, reflecting a

TABLE 3. Electrochemical data ^a

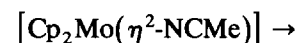
Compound	ΔE _p (mV)	$\frac{1}{2}(E_{p_a} + E_{p_c})$ (V)	i _c /i _a
[Cp ₂ MoMe(PMe ₃)]PF ₆ (3a)	50	0.68	1
[Cp ₂ MoEt(PMe ₃)]PF ₆ (3b)	50	0.67	1
[Cp ₂ MoMe(PPh ₃)]PF ₆ (7)	80	0.75	1.01
[Cp ₂ MoMe(CNMe)]I (4a)	50	0.88	1
[Cp ₂ MoEt'(CNMe)]I (4b)	50	0.86	1

^a Cyclic voltammetry was performed at room temperature on 10^{–3} M solutions of the complex in MeCN and [ⁿBu₄N]PF₆ (0.10 M; the supporting electrolyte) at a scan rate of 100 mV s^{–1}.

higher electronic density on the metal. The PPh₃ ligand is intermediate between PMe₃ and CNMe. On the other hand, no difference between the potentials of the Me and Et derivatives is observed unlike the complexes [Cp₂MoR₂] where the difference in the oxidation potentials for R = Me and Et is about 60 mV [2]. The reason for this unexpected behaviour is not easy to identify. However, as noted elsewhere [1a], the complexes [Cp₂MoR(L)]⁺ have a lower symmetry than [Cp₂MoMe₂] owing to the distortions caused by the different ligands L. Since the anomalously low oxidation potential of the latter complex originates in an antibonding interaction between C–H bonds and the HOMO [2], it is likely that this distortion, affecting the orbital symmetry, relieves the antibonding situation, leading to normal values for the potentials. No significant difference between the oxidation potentials is observed for the diethyl and dibutyl derivatives, which do not suffer the anomalous destabilization observed for the dimethyl derivative. Accordingly, no such difference is observed for [Cp₂MoR(L)]⁺ (R = Me or Et).

2.2. Oxidative additions to [Cp₂Mo(η²-NCMe)] (1)

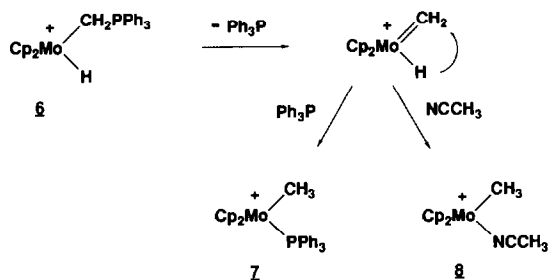
The easy preparation of **1** and the lability of the NCMe ligand in both the Cp₂Mo^{II} and Cp₂Mo^{IV} derivatives suggest that the oxidative addition of RE–ER should lead to NCMe replacement according to



This is indeed the case, since reaction of [Cp₂Mo(η²-NCMe)] in acetonitrile with Et₂S₂, Ph₂Se₂ or (PhCOO)₂ at about 50°C gives the corresponding [Cp₂Mo(ER)₂] (ER = SEt, SePh or OOCPh) in very good yield. This process provides a synthetic route to [Cp₂Mo(SePh)₂] much more attractive than the one previously reported from [Cp₂MoCl₂] and RSeLi [16]. However, this type of oxidative addition is not always observed and the reaction of **1** with PhSSiMe₃ leads to the known [Cp₂Mo(H)SPh] [17] as the only isolable product (85% yield). Similar hydride formation has also been observed in the reaction of [Cp₂MoPPh₃] with Me₃SiCl [1a].

2.3. Preparation of [Cp₂MoHR] and related studies

Reaction of [Cp₂MoHI] with LiMe in tetrahydrofuran (THF) at –80°C followed by warming to –30°C and further work-up at or below this temperature gave yellow pentane-soluble [Cp₂Mo(H)Me] (**5**) in good yield. In contrast, reaction of [Cp₂MoXMe] (X = Cl or Br) [2] with Red-Al gave only [Cp₂MoH₂]. The alkyl hydride **5** is rather thermally sensitive, particularly in solution. Its ¹H NMR spectrum at –30°C in toluene-

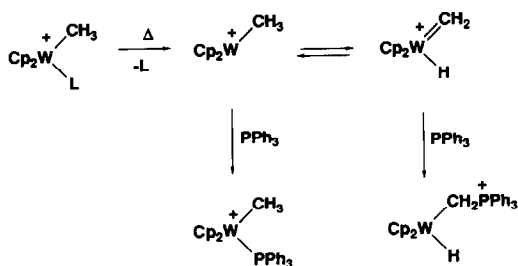


Scheme 1.

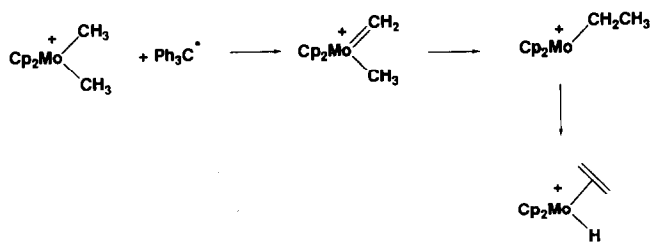
d_8 (Table 1) shows the expected singlet resonances at 0.32 ppm (Mo-CH₃) and -8.89 ppm (Mo-H). Above -20°C decomposition is observed and at -10°C these resonances disappear, but no definite product could be identified. In the solid state the stability was just enough to get a reproducible C, H analysis from freshly purified samples. In view of its instability and difficult preparation, no further attempts were made to study its reactivity and/or decomposition. Nevertheless, the three compounds [Cp₂MoH₂] (decomposition above 200°C), [Cp₂MoMe₂] (decomposition at 180°C) and [Cp₂MoH(Me)] are another demonstration of the enhanced instability of *cis* H-alkyl fragments compared with their *cis* dihydride and dialkyl analogues.

The reaction of [Cp₂MoHI] and H₂CPPH₃ affords [Cp₂Mo(H)CH₂PPh₃]⁺ (6) isolated as the THF solvate in 91% yield. In contrast with [Cp₂MoHMe], 6 is stable at room temperature and the ¹H NMR spectrum shows the expected Mo-CH₂-P doublet and Mo-H resonances (Table 1).

Heating a solution of 6 in NCMe for 6 h under reflux followed by work-up with NH₄PF₆ gives a crude precipitate. The ¹H NMR spectrum shows that it is a mixture of [Cp₂MoMe(PPh₃)]⁺ (7) and [Cp₂MoMe(NCMe)]⁺ (8), both of which are already known [18]. The formation of 7 and 8 in good yields excludes reductive elimination of [CH₃PPh₃]⁺ as the dominant pathway and no salt of this cation could be isolated from the reaction mixture. The alternative decomposition mode can be understood from the mechanism shown in Scheme 1, which is initiated by PPh₃ dissociation



Scheme 2.



Scheme 3.

tion and H migration to the adjacent methylidene. The external ligand, either PPh₃ or NCMe, occupies the vacant coordination site to give 7 or 8 respectively.

In essence, this mechanism is the reverse reaction of α elimination from [Cp₂WMe(L)]⁺ where L is a labile ligand (Scheme 2) [19].

Given the general similarities between molybdenocene and tungstenocene, this result is rather predictable, but to our knowledge no evidence for (CH₂) derivatives of molybdenocene has yet been produced. Indeed, similar α elimination has been observed on irradiation of [Cp₂WMe₂]⁺ in NCMe + PPh₃ to give [Cp₂W(H)(CH₂PPh₃)]⁺ after initial loss of CH₃[•] radicals [20], but the same reaction with [Cp₂MoMe₂]⁺ gave 8 without any evidence of a methylidene complex [18].

Further proof of the transient existence of [Cp₂Mo=CH₂]⁺ is given by the reaction of [Cp₂MoMe₂]PF₆ with Ph₃C⁺, which leads to [Cp₂MoH(C₂H₄)]⁺ in high yield as depicted in Scheme 3. The analogous experiment with W was reported by Hayes *et al.* [21].

3. Experimental details

3.1. Syntheses

All experiments were carried out under an atmosphere of argon using Schlenk techniques. Solvents (diethyl ether, toluene and THF) were dried by distillation from Na + benzophenone. Acetonitrile was dried over CaH₂ and distilled after refluxing for several hours over P₂O₅. Acetone was distilled and kept over 4 Å molecular sieves. [Cp₂Mo(η^2 -NCMe)] [3], [Cp₂MoR(CNMe)]I (R = Me or Et) [1c], [Cp₂Mo(PPh₃)] and [Cp₂MoMe(PPh₃)]PF₆ [1a] were prepared as described in the literature.

3.2. Analytical procedures

Microanalyses were performed by Dornis and Kolbe Microanalytical Laboratory, Mülheim/Ruhr, Germany and in our laboratories.

¹H NMR spectra were obtained with JEOL JN-PS-100 (100 MHz), Bruker SY 80 FT (80 MHz) and Bruker CXP 300 (300 MHz) spectrometers. IR spectra

were recorded on a Perkin–Elmer 457 spectrophotometer using KBr pellets.

3.3. Crystal structure determination

Crystal data: $C_{13}H_{19}MoP$, $M_r = 302.21$, orthorhombic, space group $Cmc2_1$, $a = 12.750(4)$, $b = 10.504(2)$, $c = 9.293(6)$ Å, $V = 1244.6$ Å³, $Z = 4$, $D_c = 1.61$ g cm⁻³, $\mu(Mo K\alpha) = 10.32$ cm⁻¹.

Data collection: All X-ray measurements were made at room temperature using an Enraf–Nonius CAD4 diffractometer and graphite-monochromatized Mo K α radiation ($\lambda = 0.71069$ Å). The intensities of 1831 unique reflections in the range $1.5^\circ \leq \theta \leq 30.0^\circ$ were measured in the ω – 2θ scan mode with ω scan widths of $0.80 + 0.35 \tan \theta$. The data were empirically corrected for absorption using the Enraf–Nonius CAD4 software (minimum and maximum transmission factors of 0.8592 and 0.9967 respectively).

Structure determination and refinement: 1726 reflections satisfied the criterion $F \geq 3\sigma(F)$ and were used for structure solution and refinement. The molybdenum position was located on a mirror plane from a Patterson map and the positions of the other non-hydrogen atoms from subsequent difference Fourier syntheses. The phosphorus atom and carbon C(2) also lie on the same plane as Mo. The hydrogen atoms were calculated and inserted in idealized positions. All non-hydrogen atoms were refined anisotropically. The weighting scheme $w = (1.208/\sigma^2) |F| + 0.000416F^2$ was found to give acceptable agreement analysis. Six low angle and strong reflections thought to be affected by extinction were removed from the data. The final refinement converged at $R = 0.0285$ and $R_w = 0.0290$. The maximum shift/e.s.d. ratio in the final refinement cycle was 0.007. A peak of $1.62 e \text{ \AA}^{-3}$ in the vicinity of the molybdenum atom remained in the final electron density difference map. A comparative refinement with all atoms in the molecule in the $(-x, -y, -z)$ positions converged to $R = 0.0303$ and $R_w = 0.0310$, thereby confirming the initial absolute configuration

for the molecule now reported. Final atomic positional parameters for the refined atoms are presented in Table 4.

Anisotropic displacement factors, coefficients and positional parameters for idealized hydrogen as well as lists of observed and calculated structure factors are available as supplementary data from the authors and deposited. All computations required to solve and refine the structure were done using SHELX86 [22] and SHELX76 [23]; the drawing was done using ORTEP [24].

3.4. Electrochemistry

The electrochemical instrumentation consisted of a PAR 173 potentiometer, a PAR 175 voltage programmer and a Houston Instruments Omnigraphic 2000 X–T. Potentials were referred to a calomel electrode (SCE) containing a saturated solution of KCl. The experimental set-up was checked against a 10^{-3} M solution of ferrocene and LiClO₄ (0.10 M) in acetonitrile. The ferrocenium/ferrocene potential was in agreement with the literature value [25].

The working electrodes were a 2 mm piece of Pt wire and the auxiliary electrode a Pt wire coil. The experiments were performed in a PAR polarographic cell at room temperature. The solutions used were 1 mM in solute and 0.1 M in supporting electrolyte, tetrabutylammonium hexafluorophosphate.

Solvents were dried as described above. Solutions were degassed with dry N₂ before each experiment and an N₂ atmosphere was maintained over the solution during the experiments.

Preparation of $[Cp_2Mo(PMe_3)]$ (2)

PMe₃ (1 ml) was added to a solution of $[Cp_2Mo(\eta^2\text{-NCMe})]$ (0.160 g, 0.60 mmol) in toluene. The reaction mixture was stirred for 6 h at 60°C, the solvent evaporated in vacuum and the residue extracted with diethyl ether at 40°C. The compound was obtained as red crystals by cooling the extract. Yield 60%. Anal. Found: C, 51.57; H, 6.32; Mo, 31.70; P, 10.16. $C_{13}H_{19}MoP$ calc.: C, 51.62; H, 6.34; Mo, 31.74; P, 10.26.

Preparation of $[Cp_2MoMe(PMe_3)]PF_6$ (3a)

Addition of MeI (40 μ l) to a solution of $[Cp_2Mo(PMe_3)]$ (0.158 g, 0.53 mmol) in 20 ml toluene caused immediate precipitation of a yellow solid. This was filtered off, washed with Et₂O (3 \times 5 ml), taken up in 30 ml H₂O and treated with aqueous NH₄PF₆. The resulting precipitate was filtered, washed with H₂O and recrystallized from acetone + Et₂O to give orange crystals in 70% yield. Anal. Found: C, 36.22; H, 4.71; P, 12.70. $C_{14}H_{22}F_6MoP_2$ calc.: C, 36.34; H, 4.80; P 13.41. IR, ν_{\max} (KBr): 3110, 2980, 2900, 2810, 1440, 1320 and 830 cm⁻¹.

TABLE 4. Positional parameters

	x	y	z
Mo	0	8121.3(3)	10000
P(1)	0	6645(1)	7932(2)
C(11)	1152(3)	9284(4)	11316(4)
C(12)	1394(3)	9480(4)	9820(6)
C(13)	1705(3)	8292(4)	9284(5)
C(14)	1652(3)	7348(4)	10404(5)
C(15)	1287(3)	7962(4)	11663(5)
C(1)	-1093(4)	5529(5)	7730(7)
C(2)	0	7324(8)	6133(7)

Preparation of $[Cp_2MoEt(PMe_3)]PF_6$ (3b)

Treatment of a solution of $[Cp_2Mo(PMe_3)]$ (0.444 g, 1.47 mmol) in 40 ml toluene with EtI (130 μ l) caused immediate precipitation of a yellow solid. This was filtered off, washed with Et₂O (2 \times 3 ml), taken up in 30 ml H₂O and treated with aqueous NH₄PF₆. The resulting precipitate was filtered, washed with H₂O and recrystallized from acetone + Et₂O to give orange crystals in 70% yield. Anal. Found: C, 37.80; H, 5.06; Mo, 20.10; P, 12.99. C₁₄H₂₄F₆MoP₂ calc.: C, 37.83; H, 5.08; Mo, 20.14; P, 13.02. IR, ν_{max} (KBr): 3110, 2980, 2880, 1440, 1320 and 830 cm⁻¹.

Reaction of $[Cp_2Mo(\eta^2-NCMe)]$ with Et₂S₂

A solution of $[Cp_2Mo(\eta^2-NCMe)]$ (0.145 g, 0.54 mmol) in MeCN was treated with Et₂S₂ (2 ml) for 2 h at 45°C. The solution was evaporated to dryness and the orange residue washed with Et₂O (3 \times 5 ml) and shown to be $[Cp_2Mo(SET_2)]$ (80% yield) by comparison of its IR and ¹H NMR spectra with those of an authentic sample [26].

Reaction of $[Cp_2Mo(\eta^2-NCMe)]$ with Ph₂Se₂

$[Cp_2Mo(\eta^2-NCMe)]$ (0.145 g, 0.54 mmol) was dissolved in MeCN and treated with Ph₂Se₂ (0.175 mg, 0.56 mmol). The reaction mixture was stirred for 2 h. The resulting precipitate was filtered off, washed with Et₂O (3 \times 7 ml) and shown to be $[Cp_2Mo(SePh)_2]$ [16] (60% yield). Anal. Found: C, 49.80; H, 3.73; Mo, 17.80. C₂₂H₂₀MoSe₂ calc.: C, 49.10; H, 3.75; Mo, 17.82. IR, (KBr): 3100, 1570, 1475, 1440, 750 and 700 cm⁻¹.

Reaction of $[Cp_2Mo(\eta^2-NCMe)]$ with (PhCOO)₂

(PhCOO)₂ (0.102 g, 0.42 mmol) was added to a solution of $[Cp_2Mo(\eta^2-NCMe)]$ (0.110 g, 0.41 mmol) in MeCN and stirred for 1 h. A grey precipitate separated and the solution became brown. The precipitate was filtered off and the solution evaporated. The oily residue was washed with diethyl ether. Recrystallization from CH₂Cl₂ + Et₂O afforded $[Cp_2Mo(OCOPh)_2]$ as a brown powder in 60% yield by comparison of its IR and ¹H NMR spectra with those of an authentic sample [26].

Preparation of $[Cp_2Mo(H)Me]$ (5)

$[Cp_2Mo(H)I]$ (0.30 g, 0.86 mmol) was dissolved in THF at -80°C and LiMe in Et₂O (2.0 ml, 3.6 mmol) was added. The reaction mixture was allowed to warm to -30°C and unreacted LiMe destroyed with a few drops of ethanol. The solvent was removed in vacuum at -30°C and the residue extracted with pentane. Cooling the concentrated extract at -80°C for 40 h gave the product as a yellow powder in 40% yield. Anal. Found: C, 54.38; H, 5.84. C₁₁H₁₄Mo calc.: C, 54.56; H, 5.83.

Preparation of $[Cp_2Mo(H)CH_2PPh_3]I$ (6)

A solution of $[Cp_2Mo(H)I]$ (0.30 g, 0.87 mmol) in THF was treated with a solution of CH₂PPh₃ (0.24 g, 0.87 mmol) in the same solvent. The resulting yellow precipitate was filtered off and washed with Et₂O (3 \times 5 ml). Yield 91%. Anal. Found: C, 56.38; H, 5.42. C₃₃H₃₆IMoOP calc.: C, 56.40; H, 5.20. IR, ν_{max} (KBr): 3060, 2980, 2890, 1430, 1110, 750, 715 and 690 cm⁻¹.

4. Conclusions

The complex $[Cp_2Mo(\eta^2-NCMe)]$ is a very convenient starting material for the preparation of other $[Cp_2MoL]$ derivatives, both in the 2+, $[Cp_2MoL]$, and 4+, $[Cp_2Mo(ER)_2]$, oxidation states. The possibility of extending this addition to N-N and P-P bonds is being tested. With regard to the chemistry of alkyl hydrides and alkylidenes, the Cp₂Mo fragment behaves in a manner entirely analogous to its W analogue, although intramolecular migrations of H and R to the adjacent CH₂ are much faster, as expected.

References

- (a) C. G. de Azevedo, M. J. Calhorda, M. A. A. F. de C. T. Carrondo, A. R. Dias, V. Félix and C. C. Romão, *J. Organomet. Chem.*, 391 (1990) 345; (b) M. J. Calhorda, A. R. Dias, A. M. Martins and C. C. Romão, *Polyhedron*, 8 (1989) 1802; (c) A. M. Martins, M. J. Calhorda, C. C. Romão, C. Völkl, P. Kiprof and A. C. Fillippou, *J. Organomet. Chem.*, 423 (1992) 367.
- M. J. Calhorda, M. A. A. F. de C. T. Carrondo, A. R. Dias, A. M. Galvão, M. H. Garcia, A. M. Martins, M. E. M. da Piedade, C. I. Pinheiro, C. C. Romão, J. A. M. Simões and L. F. Veiros, *Organometallics*, 10 (1991) 483.
- T. C. Wright, G. Wilkinson, M. Motevalli and M. B. Hursthouse, *J. Chem. Soc., Dalton Trans.*, (1986) 2017.
- (a) J. L. Thomas, *J. Am. Chem. Soc.*, 95 (1973) 1838; (b) J. L. Thomas and H. H. Brintzinger, *J. Am. Chem. Soc.*, 94 (1972) 1386.
- (a) F. W. S. Benfield, B. R. Francis and M. L. H. Green, *J. Organomet. Chem.*, 44 (1972) C13; (b) F. W. S. Benfield and M. L. H. Green, *J. Chem. Soc., Dalton Trans.*, (1974) 1324.
- K. L. T. Wong, J. L. Thomas and H. H. Brintzinger, *J. Am. Chem. Soc.*, 96 (1974) 3694.
- (a) A. Nakamura and S. Otsuka, *J. Am. Chem. Soc.*, 95 (1973) 7262; (b) G. L. Geoffroy and M. G. Bradley, *J. Organomet. Chem.*, 134 (1977) C27; (c) G. L. Geoffroy and M. G. Bradley, *Inorg. Chem.*, 17 (1978) 2410; (d) J. Okuda and G. E. Herberich, *Organometallics*, 6 (1987) 2331; (e) J. M. Galante, J. W. Bruno, P. N. Hazin, K. Folting and J. C. Huffman, *Organometallics*, 7 (1988) 1066.
- N. J. Cooper, M. L. H. Green and R. Mahtab, *J. Chem. Soc., Dalton Trans.*, (1979) 1557.
- C. G. de Azevedo, A. R. Dias, A. M. Martins and C. C. Romão, *J. Organomet. Chem.*, 368 (1989) 5.
- P. B. Hitchcock, M. F. Lappert and W.-P. Leung, *J. Chem. Soc., Chem. Commun.*, (1987) 1282.
- A. H. Cowley, D. M. Giolando, C. M. Nunn, M. Pakulski, D. Westmoreland and N. C. Norman, *J. Chem. Soc., Dalton Trans.*, (1988) 2127.

- 12 I. D. Brown, M. C. Brown and F. C. Hawthorne, *Bond Index to the Determinations of Inorganic Crystal Structures*, Institute for Materials Research, McMaster University, 1969–1977.
- 13 M. M. Kubicki, R. Kergoat, M. Curiou and P. L. L'Haridon, *J. Organomet. Chem.*, 322 (1987) 357.
- 14 S. R. Allen, M. Green, G. Moran, A. G. Orpen and G. E. Taylor, *J. Chem. Soc., Dalton Trans.*, (1984) 441.
- 15 H. Adams, N. A. Bailey, J. T. Gauntlett, I. M. Harkin, M. J. Winter and S. Woodward, *J. Chem. Soc., Dalton Trans.*, (1991) 1117.
- 16 M. Satao and T. Yoshida, *J. Organomet. Chem.*, 87 (1975) 217.
- 17 M. J. Calhorda, M. A. A. F. de C. T. Carrondo, A. R. Dias, A. M. T. Domingos, M. T. L. S. Duarte, M. H. Garcia and C. C. Romão, *J. Organomet. Chem.*, 320 (1987) 63.
- 18 S. M. B. Costa, A. R. Dias and F. J. S. Pina, *J. Organomet. Chem.*, 175 (1979) 193.
- 19 N. J. Cooper and M. L. H. Green, *J. Chem. Soc., Dalton Trans.*, (1979) 1121.
- 20 S. M. B. Costa, A. R. Dias and F. J. S. Pina, *J. Chem. Soc., Dalton Trans.*, (1981) 314.
- 21 J. C. Hayes, G. D. N. Pearson and N. J. Cooper, *J. Am. Chem. Soc.*, 103 (1981) 4648.
- 22 G. M. Sheldrick, SHELX; *Crystallographic Calculation Program*, University of Cambridge, 1976.
- 23 G. M. Sheldrick, in G. M. Sheldrick, G. Krüger and R. Goddard (eds.), *Crystallographic Computing 3*, Oxford University Press, Oxford, 1985.
- 24 C. K. Johnson, ORTEP-II, *Rep. ORNL-5138*, 1976 (Oak Ridge National Laboratory, Park Ridge, TN).
- 25 I. V. Nelson and R. T. Iwamoto, *Anal. Chem.*, 35 (1963) 867.
- 26 M. G. Harriss, M. L. H. Green and W. E. Lindsell, *J. Chem. Soc. A*, (1969) 1453.